Spectroscopic and Photorefractive investigation of vanadium-doped cadmium telluride

Philippe Delaye, F. Bignon, Gérald Roosen, Jean-Paul Zielinger, Z. Guellil, Jean-Claude Launay, V. Mazoyer

Spectroscopic and Photorefractive investigation of vanadium-doped cadmium telluride

Ph. Delaye[1], F. Bignon[1], G. Roosen[1]

1) Institut d'Optique Théorique et Appliquée, Unité Associée au Centre National de la Recherche Scientifique, Centre Scientifique d'Orsay,
B.P. 147, 91403 Orsay Cedex, France.

M. Tapiero[2], J.P. Zielinger[2], Z. Guellil[2],

2) Institut de Physique et Chimie des Matériaux de Strasbourg, Unité Mixte 380046 CNRS-ULP-EHICS, 5 rue de l'Université,
67084 Strasbourg Cedex, France

J.C. Launay[3,4], V. Mazoyer[3],

3) Pôle de Recherche Aquitain pour les matériaux dans l'espace (Prame), B.P. 11, 33165 Saint Médard en Jalles Cedex, France

4) Laboratoire de Chimie du Solide du Centre National de la Recherche Scientifique, Université de Bordeaux I, 33405 Talence Cedex, France

Abstract: We present results on the characterization of semi-insulating vanadium-doped cadmium telluride crystals by different optical techniques such as photoinduced current transient spectroscopy, absorption, photoconductivity spectra and photorefractive wave mixing.

PACS: 42.65, 42.70, 72.40.

1 Introduction

The investigation of photorefractive semiconductors is strongly motivated by the compatibility of their operating wavelengths with semiconductor lasers and with fiber optics communications. For a better understanding of the complex processes occuring in photorefractive materials, a variety of research area are now involved including not only nonlinear optical properties but also crystal spectroscopy. In this context, we are pursuing the work we recently started (1) for the determination of deep trapping levels that directly affect the photorefractive properties of V doped CdTe crystals and for optimizing this crystal regarding to the key photorefractive parameters.

We have grown V-doped CdTe crystals using the modified Bridgman technique from CdTe (6-9's grade) in evacuated (10^{-6} torr) graphitized quartz ampoules (to minimize nucleation sites). The purity of vanadium was at least 5-9's grade. Crystals were grown with the dopant either added either compensated to the melt and the concentration of Vanadium was 5×10^{19}at.cm^{-3} and 1.5×10^{19}at.cm^{-3} in samples 1H and 6B respectively.

2. Spectroscopic characterization.

A number of different trap species have been detected in semi-insulating CdTe using Thermally Stimulated Current (TSC) and PhotoInduced Current Transient Spectroscopy (PICTS) techniques[2,3].However a complete and precise characterisation of deep levels over a wide range of energies was so far not possible. We have developed an improved PICTS technique which allows significant progress in this direction[4]. PICTS is a transient photoconductivity, computer based technique. The current transient (Fig. 1) induced by a square light pulse is recorded every 1K, during a temperature scan from 80 K up to 400 K. Two types of numerical processing of the stored data allow us to extract the parameters of the traps i.e. the apparent thermal ionization energy E_t, the capture cross section S_t and the concentration N_t for the dominant species. We recall here briefly the principles of the calculation.

We consider the single trap model. As usual, retrapping of thermally released carriers is neglected [4]. The trapped charge $n_t(t)$ then decays exponentially according to: $n_t(t) = N_t \exp(-t/\tau_t)$. The relaxation time depends strongly on temperature T and is related to E_t and S_t by

$$\tau_t^{-1} = A\, S_t T^2 \exp(-E_t/kT) \qquad (1)$$

where k is the Boltzmann constant and A a constant [4].

If the decaying charge is measured at two fixed delay times t_1 and t_2, the difference $\Delta n = n_t(t_1) - n_t(t_2)$ obviously goes through a maximum at a temperature T_m where τ_t takes a defined value τ_m which can be related mathematically to t_1 and t_2 using the condition for the maximum of the function $f(\tau_t)=\exp(-t_1/\tau_t) - \exp(-t_2/\tau_t)$. The important point is that τ_m can be computed knowing t_1 and t_2, whereas T_m is obtained on the curve $An_t(t)$ (hereafter called PICTS spectrum). The spectrum is plotted for a serie of couples (t_1, t_2), so that maxima at different temperatures are observed. The Arrhenius plot $\log(\tau_m T_m^2)=f(1/T_m)$ yields E_t and S_t according to (1). The height of the peak provides a measure of N_t [4].

In practice, however $n_t(t)$ is not directly accessible but through the transient current decay which can be expressed as

$$i(t) = \{B\mu\tau N_t / \tau_t\} \exp(-t/\tau_t) \qquad (2)$$

where B is a constant, μ the mobility and τ the recombination lifetime.

If $\mu\tau$ is assume to be constant [5,4], the condition for the maximum is deduced from the function: $g(\tau_t)= 1/\tau_t.[\exp(-t_1/\tau_t) - \exp(-t_2/\tau_t)]$. Actually $\mu\tau$ is temperature dependant. As a consequence this simple double-gate (DG) procedure does not yield very reliable values for the trap parameters.

A better alternative is to normalize the DG signal by the photocurrent i(0) which is proportionnal to $\mu\tau$ (NDG signal) (Fig.1). This method is of special interest for the determination of the trap concentrations [4].
A second alternative is to plot the fonction: $Y(T)= [i(t_1)-i(t_2)]/[i(t_0)-i(t_3)]$ where t_0, t_1, t_2, t_3 are properly chosen delay times (Fig.1). Again the condition for the maximum can be found mathematically [4]. This four gate (FG) data processing is a very sensitive method with high spectral resolution due to the fact that the pre exponential factor is eliminated in (2).

We performed our mesurements on two samples 1H and 6B, cut in the same ingots as the specimen used for photorefractivity analysis. Nearly the same thermal activation energy was found for both samples: ≈0.75 eV. Figure 2 shows normalized photoconductivity spectra. A main extrinsic band which drops sharply for photon energies $h\nu \approx 1.1$ eV is observed. The peak at roughly 1.5 eV corresponds to band to band transitions.
PICTS measurements were performed on both samples under different excitation conditions: with photons of energy close to the maximum of the photoconductivity spectrum (Fig.2), in the extrinsic band ($h\nu \approx 1$ eV), in both cases with different illuminations levels. In each case fairly the same results were obtained. A few representative result will be given here.
It is well known that the maximum photoconductivity near the absorption edge occurs for that wavelength $\lambda = \lambda_{max}$ corresponding to an absorption constant $\alpha_{max} \approx 1 / d$ where d is the thickness of the specimen. During the temperature scan λ_{max} was continiously adjusted to achieve maximum photoresponse. The optical generation rate G of photocarriers:
$G = \alpha_{max} \Phi_o = \Phi_o /d$ (Φ_o is the incident photons flux) (8)
is thus temperature independent and the plot of the photocurrent versus T (i(0) on Fig.1) represents the thermal variation of $\mu\tau$ (Fig.3, curve 1). Curve 2 shows a DG spectrum. Poorly resolved structure are visible. The spectrum is clearly modulated by the $\mu\tau = f(T)$ function. The NDG spectrum brings some improvement (Fig.4, curve 1) and allows the determination of the predominant traps (when high illumination is used to fill the traps). The FG spectrum undeniably provides the best spectral resolution (Fig.4, curve 2). Ten peaks are observed in the temperature interval 80K - 350K. The corresponding parameters are listed in table 1 for sample 1H.
Three of the detected centers could be involved in the photorefractive effect: P_9, P_8 and may be also P_7:at 300K the relaxation time of P_7 is of the order of 0.5s and its concentration (if one takes into account a possible error of the order of a factor 10) is

fairly close to N_{eff} = 4.3 x 10^{15} cm^{-3} found by photorefractive measurements (sect.3).

The high resistivity and the corresponding high thermal activation energy confirm that the dark fermi level is pinned by a deep level lying close to the midgap. This could be the V^{2+} / V^{3+} level. In the photorefractive effect V^{2+} and V^{3+} could act respectively as absorption centers and as traps. However charge transfer between two valence states of the same ion cannot be observed when the crystal is uniformly excited as in the PICTS experiment, since the concentration of V^{2+} and V^{3+} remain unchanged. Nevertheless the non observation of a dominant center (the concentration of P_9 and P_8 are lower than 10^{13} cm^{-3}) cannot be consider as a proof of proposed charge transfer model (V^{2+} -> V^{3+}) indeed the absorption and photoluminescence spectra of moderately V-doped CdTe and undoped CdTe are not very different [6].On the other hand the following interpretation was proposed: at low concentration (<10^{20} cm^{-3}) V occupies vacant Cd sites, at high concentration interstitial sites giving rise to a new donor level [7].

3. Photorefractive analysis by two wave mixing

We present here the absorption, photoconductivity and energy transfer measurements we have conducted on the two samples 1H and 6B.

At wavelength λ = 1.06 μm, we determined a conductivity given by:

$$1H:\ \sigma = \sigma_d + \sigma_{ph} = (1.5 + 0.7\ I_0).\ 10^{-9}\ (\Omega.cm)^{-1}$$

$$6B:\ \sigma = \sigma_d + \sigma_{ph} = (0.06 + 0.5\ I_0).\ 10^{-9}\ (\Omega.cm)^{-1}$$

where I_0 is the incident irradiance in $mW.cm^{-2}$. We see that the two samples have quite the same photoconductivity mainly due to electron transport (see below). From this value, one can estimates the electron mobility-life time product [1] $\mu\tau = 9.\ 10^{-8}$ $cm^2\ V^{-1}$. Crystal 6B is a better candidate for photorefractive use as the photoconductivity will overpass the dark conductivity at very low excitation levels (at some $mW.cm^{-2}$).

At wavelength λ = 1.32 μm, we determined a conductivity expressed as:

$$1H:\ \sigma = \sigma_d + \sigma_{ph} = (1.5 + 0.2\ I_0).\ 10^{-9}\ (\Omega.cm)^{-1}.$$

$$6B:\ \sigma = \sigma_d + \sigma_{ph} = (0.06 + 0.3\ I_0).\ 10^{-9}\ (\Omega.cm)^{-1}.$$

Considering the absorbed energy, this corresponds to nearly a 5 time drop in the photoconductivity for 1H compared to what we obtained at λ = 1.06 μm, the drop is about 2 time for sample 6B, which is similar to what is obtain on the photoconductivity spectra presented in section 2.

With the set-up we previously used for characterizing InP and GaAs[8], we have investigated the photorefractive energy transfer between two waves interfering inside

the crystal. At both λ = 1.06 and 1.32 μm, the light source was a diode pumped YAG laser. The beams were polarized +/- 45° respective to the crystal (0,0,1) axis and were propagating along (1,-1,0). The grating wave vector was along the (1,1,0) direction.

Switching both beam polarizations from + 45° to - 45° changes the sign of the photorefractive gain and thus permits to discriminate between different sources of energy transfer [9]. Our experiments show that we here get a genuine photorefractive effect.

As anticipated from photoconductivity measurements, the photorefractive gain becomes independent of the input intensity for illuminations as low as few mW.cm^{-2} in sample 6B.

The analysis of the gain dependence with the grating period provides information about the effective density of traps involved in the photorefractive effect. Considering a single deep level and two possible charge carriers, the gain expression is [10] :

$$|\Gamma| = \frac{2\pi\, n_0^3 |r_{41}|}{\lambda \cos\theta} \frac{k_B T}{e} \frac{k\left|\xi_0 k^2 + b - c\right|}{\left(k^2 + \frac{k^4}{k_0^2} + b + c\right)}$$

with:

$$k_0^2 = \frac{e^2}{\varepsilon\, k_B T} N_{eff} \qquad \xi_0 = \frac{(\alpha_n - \alpha_p)}{(\alpha_n + \alpha_p)} \qquad b = \frac{(\alpha_n \kappa_p^2)}{(\alpha_n + \alpha_p)} \qquad c = \frac{(\alpha_p \kappa_n^2)}{(\alpha_n + \alpha_p)}$$

α_n and α_p are the absorption contributions that come from electron and hole generation respectively. κ_n and κ_p are the inverse of electron and hole diffusion lengths. k represents the grating wave number and N_{eff} is the effective trap density ($N_{eff} = N^+.N^0/[N^0+N^+]$ where N^+ and N^0 are the level concentrations in the ionized and neutral states respectively).

By a direct measure of the sign of the Pockels effect and of the photorefractive gain in one fixed configuration[11], we determine that the predominant carrier for photorefractive effect at 1.06 μm is electrons for both samples.This means that we have $\alpha_n > \alpha_p$, so photoconductivity is dominated by electrons.

As now routinely done, the photorefractive gain Γ is deduced from the measurement of the amplification (attenuation) of one of the interfering beam in presence of the other.

Plotting our experimental data as k / Γ versus k^2 (Fig.5) permits the determination of the characteristic photorefractive parameters[12]. For large values of k^2, coefficients b and c are negligible and we get a straight line. Its slope and intercept at the origin give $(r_{41}\xi_0 k_0^2)^{-1}$ and $(r_{41}\xi_0)^{-1}$.

A departure from this straight line is visible for sample 1H at small values of k^2. This indicates the influence of the carrier diffusion lengths. A full fit of the experimental

data with the complete gain expression, i.e., without neglecting b and c, is now carried out using the previously determined quantities as starting parameters. We obtain:

$\xi_0 = 0.62$ +/- 0.06

$r_{41} = (5.5$ +/- 0.5) pm V^{-1}

$k_0^2 = (300$ +/- 30) μm^{-2}

$b = (3.6$ +/- 1.5) μm^{-2}

$c \approx 0$

Also known is the previously measured absorption: $\alpha = (2.16$ +/- 0.06) cm^{-1}.

Note that at a grating spacing $\Lambda = 0.9$ μm, one gets in 1H a photorefractive gain $\Gamma = 0.7$ cm^{-1} that exceeds typical gains in GaAs and InP by more than 50%[8].

For the sample 6B, the lower value of the gain prevents us to determine other coefficient than ξ_0 and k_0^2. Taking for r_{41} the value determine for sample 1H, we deduce for sample 6B:

$\xi_0 = 0.51$ +/- 0.06

$k_0^2 = (82$ +/- 20) μm^{-2}

To these results we can add the linear absorption: $\alpha = (1.00$ +/- 0.03) cm^{-1}.

These results obtain for both crystals call on the following remarks. First, the ξ_0 value indicates an electron-hole competition that is larger than previously seen in different samples[13]. Nevertheless, the photorefractive gain has an appreciable value. Second, coefficient b determined in 1H permits an estimation of the mobility-life time product of the minority carrier (i.e. holes) for the photorefractive effect; one gets $\kappa_n^2 << \kappa_p^2$ and derives for the $\mu\tau$ product of holes, $\mu\tau = 9. 10^{-8}$ cm^2 V^{-1}.

From k_0^2, we inferre the effective deep level density that contributes to the photorefractive effect, $N_{eff} = 4.3 \times 10^{15}$ cm^{-3} and $N_{eff} = 1.2 \times 10^{15}$ cm^{-3} for samples 1H and 6B respectively. As discussed in ref.14, in the low illumination quasicontinuous regime as here considered, the presence of shallow traps does not change the steady state photorefractive effect. Thus, these CW photorefractive experiments do not feel the influence of the multiple shallow traps we saw in our spectroscopic studies. It is believed that the efficient deep level for the photorefractive effect might be the P7 level identified in table 1. Considering the results presented in section 2, it appears that this density might be determined by other defects than vanadium in the CdTe 1H crystal [2,3,15].

We also conducted similar experiments at $\lambda = 1.32$ μm. First, as pointed out previously, we observed a nearly five time drop of the photoconductivity. However, for the incident illuminations used, the dark conductivity is still overpassed. Second, the magnitude of the photorefractive gain was very small in 1H ($\Gamma = 0.06$ cm^{-1} at $\Lambda = 1.5$ μm) impeding any reliable measurement versus fringe spacing. One only

estimates an electron-hole competition factor $\xi_0 = 0.1$ for 1H that corresponds to nearly balanced absorption coefficients, $\alpha_n = \alpha_p$. No gain is visible at $\lambda = 1.32$ μm in 6B.

It is clear that a contribution from multiple defects might produce such a reduction of the photorefractive gain. However, an important point we noticed, is that the photorefractive gain reverses its sign when changing the wavelength from 1.06 to 1.32 μm. This indicates a change in the nature of the photorefractive majority carrier. This result supports the approach we used for describing the photorefractive effect observed, i.e., a single deep level from which both electrons and holes are photoionized. Such a reverse in the sign of the photorefractive gain as the incident wavelength was varied, was not noticed for the crystals analyzed in ref. 16.

5. Conclusion.

We have here reported the results of our program for growth, caracterization and optimization of CdTe for photorefractive applications. High resistivity samples have been synthetized and first characterizations including spectroscopic and photorefractive ones have been made. In these samples, doped at low vanadium concentrations, a collection of defect levels has been seen, their activation energy and concentrations have been determined.

Sample 1H exhibits a fair photorefractive effect at $\lambda = 1.06$ μm with nevertheless a non negligible electron-hole competition. At $\lambda = 1.32$ μm, the effect has a reverse sign and the competition is very strong leading to a nearly full compensation. Sample 6B has a better photoconductivity over dark conductivity ratio. It exhibits a slightly lower effective "photorefractive deep level concentration" . Absorption centers may be the V_{cd}^{2-}, and the photorefractive traps could be V_{cd}^{-} (unoccupied cadmium vacancies). In this case peak P_7 can be identified to the V_{cd}^{-}. Similar characterizations are now in progress with samples more heavily V doped.

References

1_J.C.Launay, V.Mazoyer, M.Tapiero, J.P.Zielinger, Z.Guellil, Ph.Delaye, G.Roosen, Appl.Phys. **A 54**, 1992, in press

2_ C. Scharager, J.C. Muller, R. Stuck, P. Siffert, Phys. Stat. Sol. (a), **31**, 247, 1975

3_ M. Samini, B. Biglari, M. Hage-Ali, P. Siffert, J. Cryst. Grow., **72**, 213, 1985

4_ J.C. Balland, J.P. Zielinger, C. Noguet, M. Tapiero, J. Phys. D: Appl. Phys., **19**, 57, 1986; J.C. Balland, J.P. Zielinger, M. Tapiero, J.G. Gross, C. Noguet,, J. Phys. D: Appl. Phys., **19**, 71, 1986

5_R.B. Bylsma, P.M. Bridenbaugh, D.H. Olson, A.M. Glass, Appl. Phys. Lett., **51**, 889, 1987

6_N.V. Agrinskaya, O.A. Matveev, A.I. Terent'ev, V.V. Shasshkova, Sov. Phys. Semicond., **23**, 274, 1989.
7_ P.I. Babii, N.P. Gavaleshko, Yu.P. Gnatenko, P.A. Skubenko, V.I. Oleinik, Sov. Phys. Semicond., **12**, 1310, 1979
8_Ph. Delaye, P.U. Halter, G. Roosen, J. Opt.Soc.Am.B, **7**, 2268, 1990.
9_J.C. Fabre, J.M.C. Jonathan, G. Roosen, J. Opt.Soc.Am.B, **5**, 1730, 1988.
10_F.P. Strohkendl, J.M.C. Jonathan, R.W. Hellwarth, Opt. Lett. **11**, 312, 1986.
11_G.Pauliat, M.Allain, J.C.Launay, G.Roosen, Opt. Commun. **61**, 321, 1987.
12_M.B. Klein, G.C. Valley, J.Appl. Phys. **57**, 4901, 1985.
13_A. Partovi, J. Millerd, E.M. Garmire, M. Ziari, W.H. Steier, S.B. Trivedi, M.B. Klein, Appl. Phys. Lett., **57**, 846, 1990
14_G. Pauliat, G. Roosen, J. Opt. Soc. Am. B, **7**, 2259, 1990
15_A.J. Strauss, Rev. Phys. Appl., **12**, 167, 1977.
16_M. Ziari, W.H. Steier, M.B. Klein, S. Trivedi, 3rd Topical Meeting on Photefractive Materials,Beverly, 1991 Technical Digest **14**, 159.

Figure captions

Figure 1. Typical shape of the photocurrent transient induced by a square light pulse. During illumination the current rises up to a constant value i(0). The light is interrupted at time t = 0; t_0, t_1, t_2, t_3 are fixed delay times.

Figure 2. Normalized photoconductivity spectra

Figure 3. Photoconductivity versus temperature (Curve 1) and typical double gate spectrum (Curve 2)

Figure 4. Typical normalized double gate (curve 1) and four gate (curve 2) spectra.

Figure 5. Experimental Γ/k versus k^2 plot leading to the determination of the photorefractive parameters of crystals 1H and 6B. This plot was drawn with Γ in cm^{-1} and k in μm^{-1}.The dotted straight line is the fit obtained for large grating wave numbers while the full line curve represents the best fit with the whole gain expression.

TABLE 1: Parameters of the different level detected by PICTS for the sample 1H

Peak Number	E_t (eV)	S_t (cm^2)	N_t (cm^{-3})
P_0	0.25	$\approx 10^{-9}$	
P_1	0.15	10^{-16}	10^{14}
P_2	0.285	5×10^{-13}	10^{15}
P_3	0.26	4×10^{-16}	$< 10^{14}$
P_4	0.31	4×10^{-15}	8×10^{14}
P_5	0.34	10^{-16}	$< 10^{13}$
P_6	0.53	4×10^{-14}	4×10^{14}
P_7	0.62	2×10^{-14}	2×10^{14}
P_8	0.78	2×10^{-13}	
P_9	1.1	$\approx 10^{-10}$	

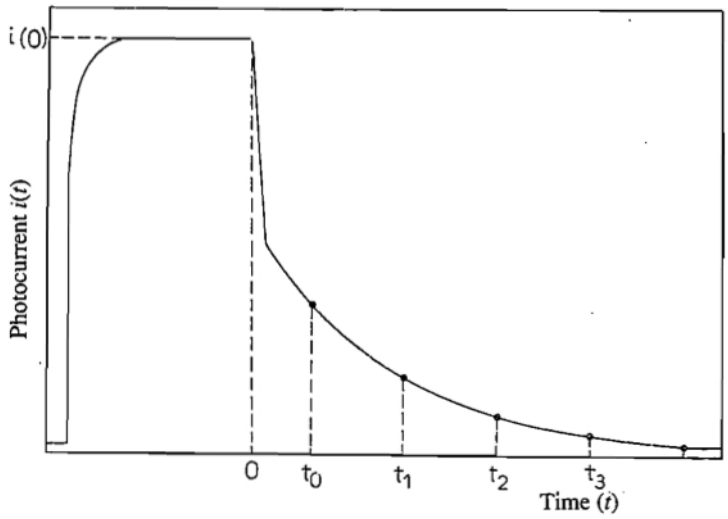

Figure 1

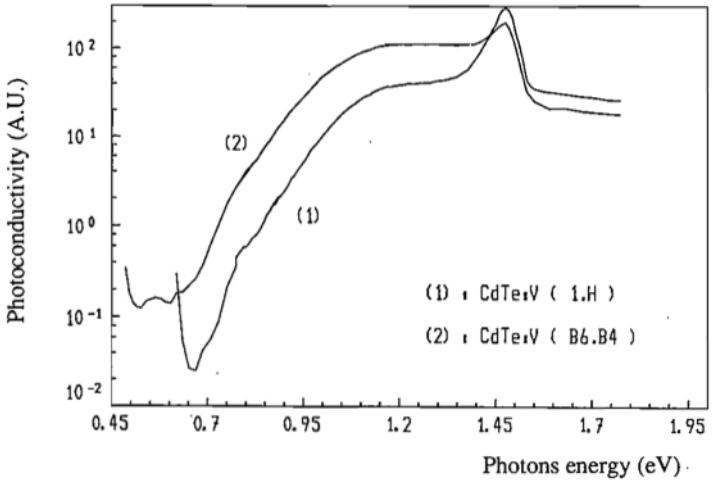

Figure 2

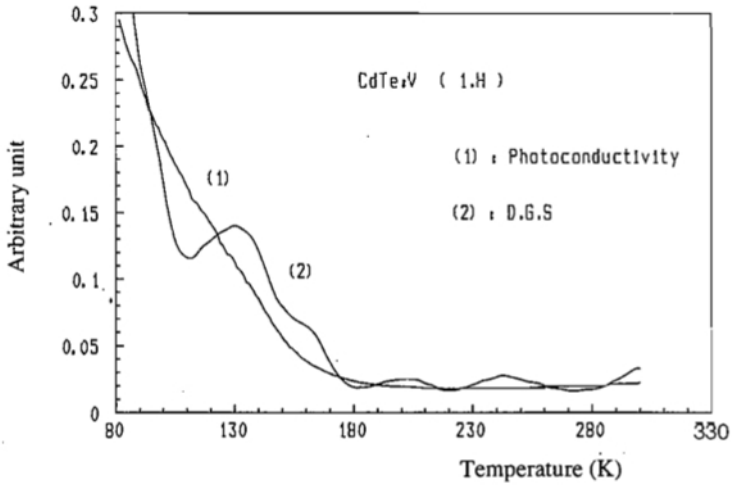

Figure 3

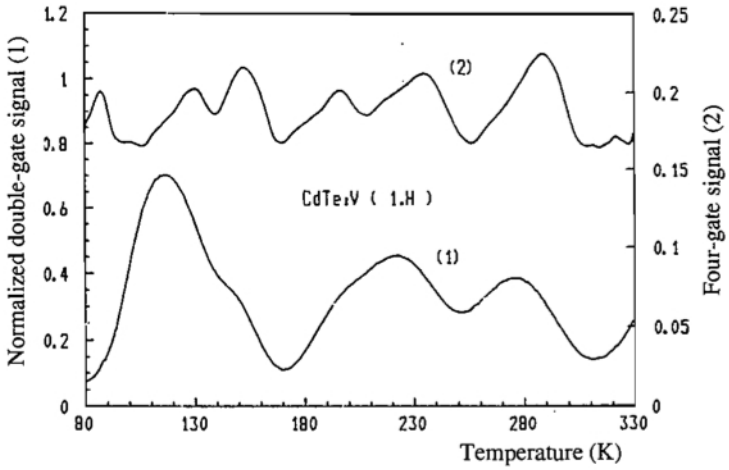

Figure 4

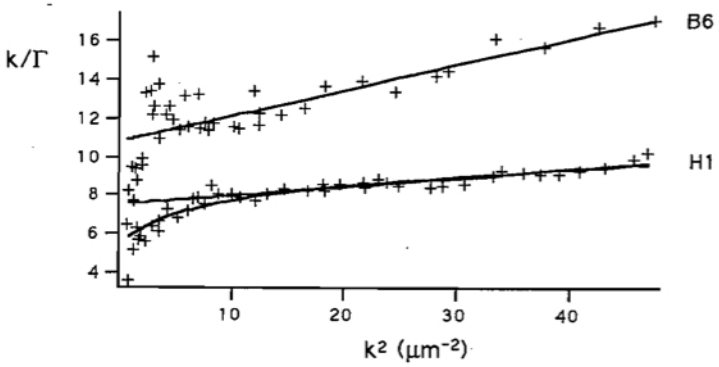

Figure 5